Understanding the activity of Zn-Cu sites in methanol synthesis

Batyrev, E.D.

Publication date
2013

Chapter 4

Detection of hydrogen–copper clustering in $Zn_{1-x}Cu_xO$ methanol synthesis catalysts using neutron scattering methods*

Abstract

The atomic and cluster structure of hydrogen-treated Cu/ZnO (the major component of methanol synthesis catalysts) was studied using Bragg powder and small-angle neutron diffraction. Isotopic substitution of Cu and H was used to obtain reliable results indicating Cu and H clustering. The clusters form on the boundaries of ZnO particles and have a complex structure: a copper cluster surrounded by an adsorbed hydrogen shell has a hydrogen core. It can be assumed that this cluster configuration has a strong effect on the catalytic activity of these compounds.

4.1 Introduction

Methanol is a starting point for producing many organic compounds, including formaldehyde, methyl methacrylate, dimethylacrylate, and others, which are of commercial importance. The efficiency and cost of these materials depend to a large extent on the efficiency and cost of production of methanol. For this reason, understanding all of the stages of the technological process of methanol production and their optimization is of particular importance.

One significant component of the technological process is the use of various catalysts, whose efficiency controls in many respects the competitiveness of the production of methanol and secondary organic compounds. After special thermal gas treatment, copper–zinc and copper–zinc–aluminum oxides are selective and active in low-pressure processes and are often used for developing efficient catalysts. Many publications have been devoted to methods and

*V.A. Trunov, A.E. Sokolov, V.T. Lebedev, O.P. Smirnov, A.I. Kurbakov, J. v.d. Heuvel, E. Batyrev, T.M. Yur'eva, L.M. Plyasova, and G. Török, *Phys. Sol. State*, 2006, 48, 1291.

techniques for these compounds; nevertheless, the nature of the catalytic activity of these compounds is not clearly understood [1–4].

It is of fundamental importance to understand the consequences of thermal treatment of a catalyst in a hydrogen atmosphere, which significantly increases the catalytic efficiency of $Zn_{1-x}Cu_xO$ compounds. Electron microscopy [5] and X-ray diffraction data [6] have indicated the formation of metallic-copper clusters. However, the question regarding the presence of hydrogen and its state and localization remain open. The problem of the nature of defects (50–150 Å in size) in the catalyst bulk that exchange copper atoms with crystallite surfaces (on which copper clusters form) during various thermal treatments also remains unsolved.

Note that there exists a critical temperature above which annealing stops the exchange of copper atoms [6] because irreversible changes occur in the defects (apparently, in their structure and composition).

To solve this problem, we performed small-angle neutron scattering (SANS) and neutron Bragg diffraction studies. To identify the copper and hydrogen in the volume of prepared samples, isotopic contrast in copper (^{63}Cu, ^{65}Cu) and hydrogen (H, D) was used, since neutron scattering is extremely sensitive to the isotopic composition in these elements.

Neutron Bragg diffraction was used to determine the matrix quality and the localization of various components in it, and small-angle neutron diffraction was used to determine the nanoscopic (superatomic) structure of the catalyst with the conditional composition $Cu_{0.08}Zn_{0.92}O[H(D)]$.

4.2 Experimental

The experiments were performed using the following setups: a Russian–French 70-detector powder diffractometer ($\Delta d/d_{hkl} \approx 0.2\%$) (LLB, Saclay, France) [7], a 48-detector powder diffractometer ($\Delta d/d_{hkl} \approx 1\%$) (Konstantinov Institute, Gatchina, Russia) [8], and Membrana-2 (Konstantinov Institute) [9] and Yellow Submarine (Institute for Solid State Physics, Budapest, Hungary) [10] small-angle scattering diffractometers.

For preliminary experiments, $Cu_{0.08}Zn_{0.92}O$ samples were prepared and annealed in a H_2 or D_2 atmosphere for 2 h at 220 °C (which will be referred to as samples H and D, respectively).

Then, based on the results of preliminary experiments, two sample series were prepared using ^{65}Cu, ^{63}Cu, H, and D isotopes. These samples have the following compositions: $^{65}Cu_{0.08}Zn_{0.92}O(H)$

(sample 1), $^{63}Cu_{0.08}Zn_{0.92}O(H)$ (sample 2), $^{65}Cu_{0.08}Zn_{0.92}O(D)$ (sample 3), and $^{63}Cu_{0.08}Zn_{0.92}O(D)$ (sample 4).

The synthesized samples were designated H65 (sample 1), H63 (sample 2), D65 (sample 3), and D63 (sample 4). All of the samples were prepared using the same technology, and the same neutron scattering experiments were carried out with each series.

Note that the results of the neutron experiments were almost identical within the experimental accuracy. This indicates reproducibility of the sample preparation technology and the absence of methodical effects in the results obtained. Therefore, there is no need to present the results for each series and we present here the results obtained with samples of the second series only.

4.3 Results

4.3.1 Preliminary experiments

Powder diffraction for samples D and H was studied using a G4.2 diffractometer (with a neutron wavelength $\lambda = 0.234$ nm) at room temperature. The results of the diffraction experiment and profile data analysis [11] (which was performed using the FullProf software [12]) are shown in Fig. 1 for sample D. Profile processing was performed using the pseudo-Voigtian (in the Thomson–Cox–Hastings version). For sample H, the diffraction spectrum is not shown, since it exhibits significantly weaker peaks, which we attribute to copper [13]. The vertical bars indicate the calculated positions of the Bragg reflections from two phases, namely, a strongly distorted ZnO structure (hexagonal crystal system, space group *P*6*3mc*) (upper bars) and copper clusters (cubic system, space group *Fm*-3*m*) (lower bars).

Possible reflections from CuO (monoclinic crystal system) and Cu_2O (orthorhombic system) are not seen in the spectrum. We also attempted to detect traces of CuH_y; however, this did not improve the profile analysis quality.

The Bragg reflections from samples D and H are significantly wider than those from pure (unmodified) ZnO. The high defect density of the $Cu_xZn_{1-x}O$ structure was also indicated in other studies, e.g., in [6]. The large reflection widths in the diffraction spectrum are apparently caused, first, by defects in the matrix bulk [5] and, second, by copper clusters on the crystallite surfaces. The problem of the actual partial substitution Cu→Zn still remains unsolved even with the use of ^{65}Cu (due to the low copper concentration and poor profile parameters of the spectrum). All of the above facts and electron microscopy data on structural defects suggest that the above chemical

formulas for the sample compositions are conditional to a large extent and that the samples are more likely solid-phase dispersions than solid solutions.

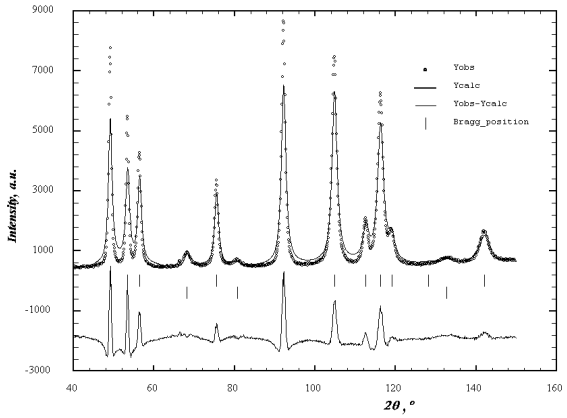

Fig. 1. *Experimental results and profile analysis of sample D.*

It is most likely that H (D) atoms are not localized in any structural positions of the ZnO matrix. All attempts to introduce hydrogen into the structure resulted in a significantly lower quality of profile fitting.

The weaker reflections from the copper phase for sample H can indicate significant localization of hydrogen atoms near copper clusters, because diffuse scattering from the hydrogen can significantly screen Bragg scattering from the copper. This is one of the main arguments in favor of performing experiments with samples prepared using the isotopes ^{65}Cu, ^{63}Cu, and D.

4.3.2 Small-angle neutron scattering study on samples with H→D substitution

Samples H and D were studied using a Membrana-2 diffractometer (neutron wavelength $\lambda = 0.3$ nm) at room temperature. To estimate multiple-scattering effects, samples of various thicknesses (1.5 and 5 mm) were studied. The transmittance was measured to be $T_{1H} = 0.91$ and $T_{1D} = 0.86$ for a sample thickness of 1.5 mm and $T_{2H} = 0.72$ and $T_{2D} = 0.77$ for a thickness of 5 mm. The sample masses were close: $M_{1H} = 0.352$ g and $M_{1D} = 0.364$ g for a thickness of 1.5 mm and $M_{2H} \approx M_{2D} = 1.7$ g for a thickness of 5 mm.

The SANS data shown in Fig. 2 for a thickness of 5 mm suggest that both protonated and deuterated samples are good

scatterers. For this reason, the measurements were performed with a rather high accuracy of ~0.1–1% in the momentum-transfer range q = 0.03–0.8 nm^{-1}.

The behavior of the scattered neutron intensity $I(q)$ is typical of polydisperse systems and is described with good accuracy by a sum of Guinier scattering functions [14]:

$$I(q) = \sum I_{0i}\exp[-q^2 R_{Gi}^2/3] + B, \quad (1)$$

where i = 1, 2, 3 labels the scattering components of the polydisperse system, R_{Gi} are the gyration radii, and I_{0i} are the partial intensities in the small-q limit for the i^{th} group of scattering particles. The constant B describes the contribution from incoherent scattering and from scattering by objects with sizes $R \leq 1$ nm.

The scattering curves shown in Fig. 2 correspond to a polydisperse medium containing three groups of particles with sizes $R \leq 2$ nm, $R \sim 2$–100 nm, and $R \sim 100$–200 nm [15].

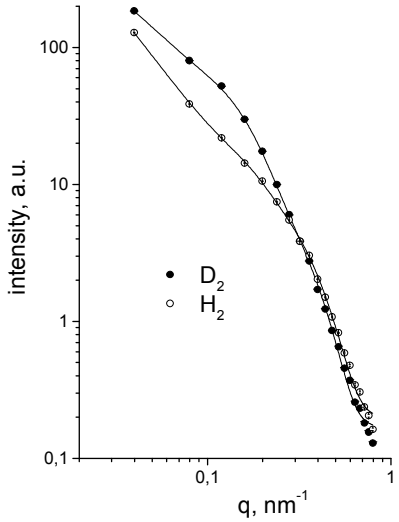

Fig. 2. *Small-angle neutron scattering on the samples D and H (layer thickness d = 5 mm). The approximation by Guinier function is shown (1). The same results were obtained for the layer with thickness d = 1.5 mm.*

The table lists the results of processing of the curves shown in Fig. 2. We can see that particles with a characteristic size $R_{G2} \sim 13$ nm provide a significant isotopic contrast, while the isotopic contrast for the two other groups of particles is significantly smaller. This

suggests that the difference intensity can be fitted well by a single-mode Guinier function,

$$I_D - I_H = \Delta I_{DH} = \Delta I_0 \exp[-q^2 R_G^2/3], \quad (2)$$

where $R_{G(H,\,D)}$ = 12.4 nm is the gyration radius (which is identical for both sample thicknesses). In the scattering-sphere approximation, the sphere radius is found to be $R_r \sim R_G\sqrt{(5/3)} \sim 16$ nm. This value is comparable to that obtained from tunneling electron microscopy data [5].

The validity of the single-mode Guinier approximation for describing ΔI_{DH} is demonstrated by the results shown in Fig. 3. Thus, the results of our preliminary experiments allowed several conclusions that are important for further experiments.

(i) The Bragg diffraction experiments confirmed the existence of metallic copper inclusions in samples exposed to a hydrogen atmosphere.

(ii) The Bragg diffraction experiments apparently indicate that hydrogen is localized near copper inclusions; it would be expedient to determine the details of this process.

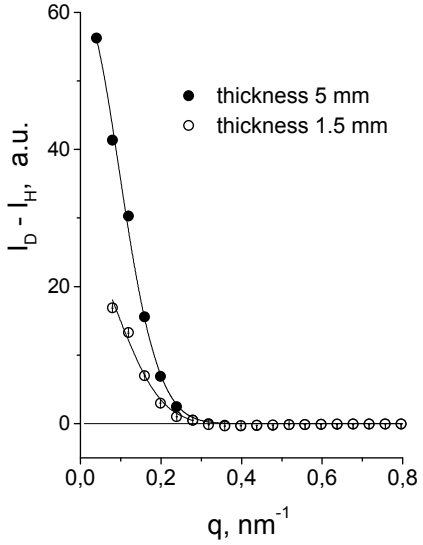

Fig. 3. *Scattered-neutron intensity differences for samples D and H with thicknesses of 1.5 and 5 mm. The data are fitted with a Guinier function.*

(iii) The small-angle scattering experiments were found to be highly sensitive to isotopic substitution and to provide an opportunity for determining the nanoscopic parameters of catalysts.

All these factors suggest the necessity of performing a more comprehensive experiment with samples containing the four isotopes (their respective nuclear coherent scattering lengths are given in parentheses): ^{63}Cu ($b_{coh} = 0.643 \times 10^{-12}$ cm), ^{65}Cu ($b_{coh} = 1.061 \times 10^{-12}$ cm), H ($b_{coh} = -0.374 \times 10^{-12}$ cm), and D ($b_{coh} = 0.6674 \times 10^{-12}$ cm).

Parameters of the scattering function in Eq. (1)

Parameter	d = 1.5 mm		d = 5.0 mm	
	H	D	H	D
I_1, arb. units	125.1 ±3.1	136.8 ±19.8	197.5 ±4.9	254.8 ±34.6
R_{G1}, nm	37.3 ±3.1	44.4 ±3.8	37.5±0.9	45.1 ±3.40
I_2, arb. units	16.1 ±1.3	45.5 ±1.9	24.9 ±2.0	93.3 ±2.7
R_{G2}, nm	13.0 ±0.7	13.4 ±0.4	13.1 ±0.7	13.2 ±0.3
I_3, arb. units	6.04 ±0.47	7.78 ±0.78	11.78 ±0.87	12.81 ±1.17
R_{G3}, nm	5.5 ±0.2	6.2 ±0.2	5.8 ±0.1	6.2 ±0.2
B, arb. units	0.13 ±0.02	0.10 ±0.01	0.20 ±0.03	0.17 ±0.02

4.4 Experiments with catalysts H65, H63, D65, and D63

Bragg diffraction experiments with sample D65 were performed using a 48-detector diffractometer [7] and confirmed the presence of copper clusters [13]. A more complete structural identification was not carried out.

Before discussing the results of experiments with doubly isotope-substituted samples, it would be expedient to present the formulas that were used to determine the parameters of the disperse nanostructure of the catalyst.

The preliminary experiments showed that using the difference intensities simplifies the problem and that it suffices to consider only single-mode disperse systems. The scattered-neutron intensity differences are defined by the difference between the partial neutron scattering cross sections. For example, the scattered-neutron intensity difference for samples H65 and H63 is given by

$$\Delta I_{H65,\,63} = I_{H65} - I_{H63} \sim \Delta\sigma_{H65,\,63}, \qquad (3)$$

where $\Delta\sigma_{H65,63}$ is the difference between the partial neutron scattering cross sections for samples H65 and H63. Like Eq. (3), the other scattered-neutron intensity differences for the samples under study can be written as

$$\Delta I_{D65,\,63} = I_{D65} - I_{D63} \sim \Delta\sigma_{D65,\,63}, \quad (4)$$

$$\Delta I_{65DH} = I_{D65} - I_{H65} \sim \Delta\sigma_{65DH}, \quad (5)$$

$$\Delta I_{63DH} = I_{D63} - I_{H63} \sim \Delta\sigma_{63DH}, \quad (6)$$

In what follows, the partial cross sections are used to analyze the experimental data.

The differences between the partial cross sections can be written as

$$\Delta\sigma_{65DH} = N_{Cl}(b_D - b_H)Y(q) \times [2b_{Cu65ef}X(q) + (b_D + b_H)Y(q)], \quad (7a)$$

$$\Delta\sigma_{D65,\,63} = N_{Cl}(b_{Cu65} - b_{Cu63})Y(q) \times [(b_{Cu65ef} + b_{Cu63ef})X(q) + (2b_D Y(q))], \quad (7b)$$

where $b_{Cu65(63)ef} = b_{Cu65(63)} - b_{ZnO}(V_{Cu}/V_{ZnO})$ is the effective scattering length of copper; V_{Cu} and V_{ZnO} are the volumes per Cu atom and per ZnO molecule, respectively; $b_{Cu65ef} = 0.49 \times 10^{-12}$ cm; $b_{Cu63ef} = 0.07 \times 10^{-12}$ cm; N_{Cl} is the number of copper clusters; and

$$X(q) = N_{Cu}F_{Cu}(q),\ Y(q) = N_{H(D)}F_{H(D)(}q). \quad (7c)$$

Here, N_{Cu} and $N_{H(D)}$ are the numbers of copper and hydrogen (deuterium) atoms in the respective clusters and F_{Cu} and $F_{H(D)}$ are the form factors of copper and hydrogen (deuterium) clusters, respectively.

From Eqs. (7a) and (7b), it follows that

$$\varepsilon(\Delta\sigma_{65DH}/\Delta\sigma_{D65,\,63}) = \chi(q) = \xi(q)[1 + \mu\xi(q)]/[1 + \delta\xi(q)], \quad (8)$$

where $\varepsilon = 0.23$, $\mu = 0.3$, $\delta = 2.39$, and $\xi(q) = Y(q)/X(q)$.

Expressions (7a), (7b), (5), and (4) are qualitatively different: Eqs. (7a) and (5) characterize the hydrogen distribution to a greater extent, and Eqs. (7b) and (4) characterize the copper distribution.

The data on the differences between the partial cross sections as obtained by analyzing the difference intensities are shown in Figs. 4 and 5.

By performing the Fourier transform of these data in the approximation of independently scattering spherically symmetric particles, we calculated the correlation functions characterizing the radial distributions of copper and hydrogen in clusters:

$$\gamma(R) = (1/2\pi^2)\int [b^{-2}(d\sigma/d\Omega)][\sin qR/(qR)]q^2 dq = \langle C(R)C(0)\rangle - \langle C(0)\rangle^2, \quad (9)$$

where $C(R)$ is the concentration of copper or hydrogen atoms as a function of radius R and b is the coherent scattering length of the corresponding isotope.

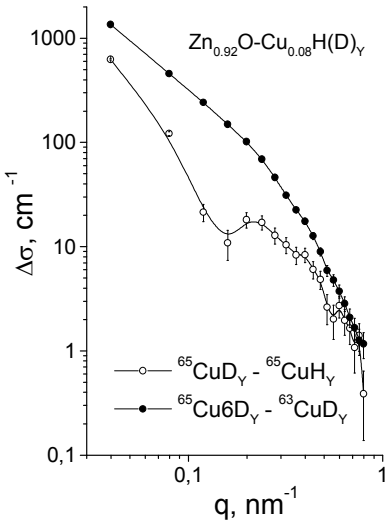

Fig. 4. *Cross section differences calculated from experimental scattered neutron intensities measured using a Membrana-2 diffractometer.*

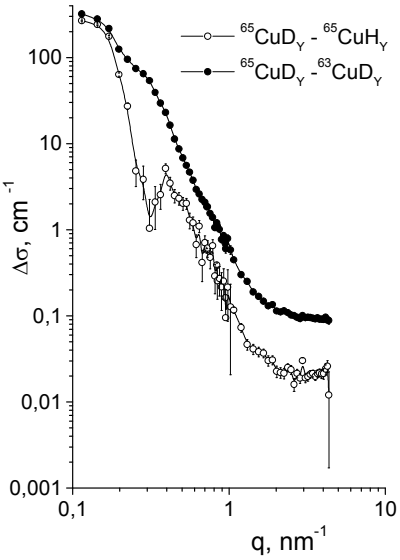

Fig. 5. *Same as in Fig. 4 but measured using the Yellow Submarine diffractometer, please note a different q range from Fig. 4.*

The calculations were carried out using the ATSAS software [16] developed at the Shubnikov Institute of Crystallography (Russian Academy of Sciences) and based on the regularization method.

4.5 Summary

The calculated correlation functions are shown in Fig. 6. We see that the hydrogen distribution is shifted to small values of *R*. This effect suggests that hydrogen occupies two different positions: (i) near defects in the ZnO matrix volume (this hydrogen can occupy only a fraction of the volume defect due to the small correlation radius) and (ii) on the surface of a defect near a copper cluster. These two coupled defects can form an electrochemical pair and cause Cu–H exchange, whose effective direction depends on the composition and temperature

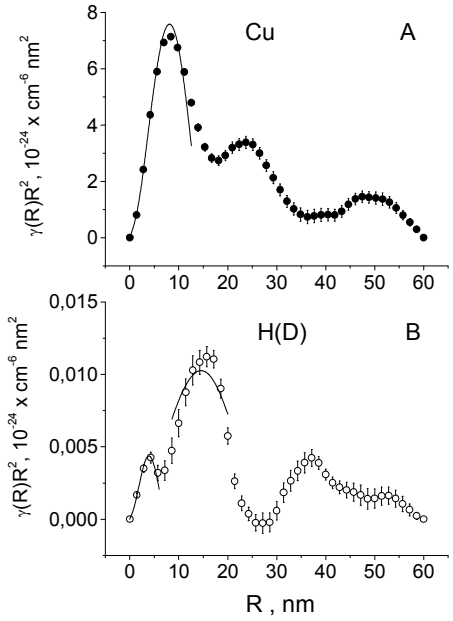

Fig. 6. *Partial correlation functions for (A) copper and (B) hydrogen (deuterium). The solid curves are fits to the model of spherical particles.*

of the gas medium into which the catalyst is placed. Such pairs cause the decomposition of molecular hydrogen into atomic hydrogen involved in the methanol synthesis reaction. It seems that there exists an equilibrium H^+ concentration between surface and bulk defects

under steady state conditions. The model of such a coupled defect is shown in Fig. 7.

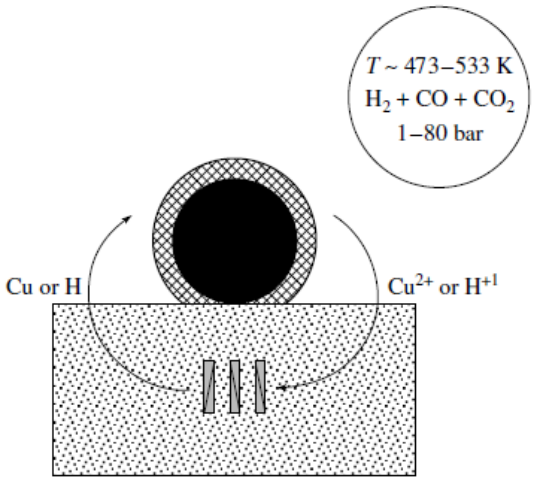

Fig. 7. *Model of a defect pair consisting of a copper cluster and a bulk defect.*

It is of interest to study the chemical composition of the bulk defect. We can assume that the chemical composition of the compound forming the defect is $Cu_{1-x-y}Zn_xH_y(OH)_2CO_3$, which is similar to the composition of malachite. Indeed, pure malachite has a decomposition temperature of ~500 K in air at normal pressure. Partial substitution of zinc can increase the decomposition temperature.

We can also assume that the neutron scattering by hydrogen localized near copper clusters and by hydrogen on bulk defects exhibits different temperature dependences. Above all, this difference can be caused by the fact that the volume of hydrogen localized on a ZnO matrix defect is small.

Preliminary experiments using the Yellow Submarine SANS diffractometer were carried out with a $ZnOCu_xH_y$ sample. It was detected that the neutron scattering from the different parts of the hydrogen subsystem exhibits significantly different behavior as the temperature is decreased. As seen in Fig. 8, the temperature dependences of neutron scattering at small values of the momentum transfer q (scattering by hydrogen localized near copper clusters) and at large q (scattering by hydrogen on bulk defects) differ significantly.

The results obtained suggest that further experiments should be performed at low temperatures down to ~2 K.

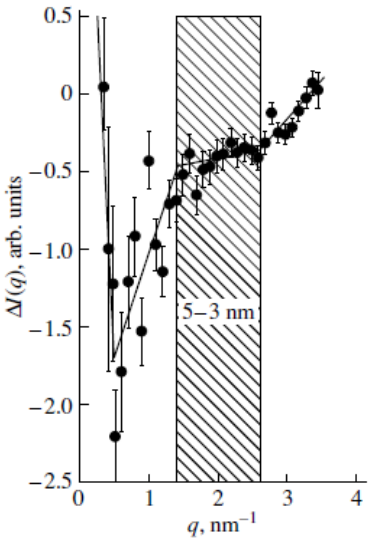

Fig. 8. *Scattered-neutron intensity differences at 100 K and room temperature. Small values of q correspond to scattering by hydrogen localized near copper clusters, and large values of q (shaded area) correspond to scattering by hydrogen on bulk defects.*

Acknowledgments

This study was supported by the Nederlandse Organisatie voor Wetenschappelijk Onderzoek in framework of NWO #047.015.004 project.

References

1. J.E. Bailie, C.H. Roches, and G.J. Millar, *Catal. Lett.*, 1995, 31, 333.
2. J. Nakamura, I. Nakamura, T. Uchijma, Y. Kanai, T. Watanabe, M. Saito, and T. Fujitani, *Catal. Lett.*, 1995, 31, 325.
3. N.M. Vijtanen, W.P.A. Jansen, R.G. van Welzeniset, H.H. Brongersma, D.S. Brands, E.K. Poels, and A. Bliek, *J. Phys. Chem. B*, 1999, 103, 6025.
4. C. Kiener, M. Kurtz, H. Wilmer, C. Hofman, H.-W. Schmidt, J.-D. Grundwaldt, M. Muhler, and F. Schuth, *J. Catal.*, 2003, 216, 110.
5. T.M. Yurieva, L.M. Plyasova, V.I. Zaikovskii, T.P. Minyukova, A. Bliek, J.C. van den Heuvel, L.P. Davydova, I.Yu. Molina, M.P.

Demeshkina, A.A. Khassin, and E. Batyrev, *Phys. Chem. Chem. Phys.*, 2004, 18, 4522.
6. L.M. Plyasova, T.M. Yurieva, T.A. Kriger, O.V. Makarova, V.I. Zaikovskii, L.P. Solovieva, and A.N. Shmakov, *Kinet. Catal.*, 1995, 36, 464.
7. A.I. Kurbakov, V.A. Trounov, T.K. Baranova, A.P. Bulkin, R.P. Dmitriev, Ya.A. Kasman, J. Rodriguez-Carvajal, and T. Roisnel, *Mater. Sci. Forum*, 2000, 321, 308.
8. I.V. Golosovskii, V.P. Kharchenkov, A.P. Bulkin, Ya.A. Kasman, V.I. Petrova, V.P. Plakhtii, V.A. Priemyshev, V.A. Trunov, É.I. Fedorova, and V.A. Tyukavin, *Preprint No. 1374, LIYaF (Leningrad Institute of Nuclear Physics, Russian Academy of Sciences, Gatchina)*, 1988.
9. M.M. Agamalyan, G.M. Drabkin, D.I. Svergun, and L.A. Feigin, *Preprint No. 1599, PNPI (St. Petersburg Institute of Nuclear Physics, Russian Academy of Sciences, Gatchina)*, 1990.
10. Ed. by L. Fragnod, L. Rosta, Gy. Török, *Neutron Scattering Facilities at Budapest Modernized Reactor (Central Research Institute for Physics of Hungarian Academy of Sciences, Budapest)*, 1991, 26.
11. H. M. Rietveld, *Acta Crystallogr.*, 1967, 22, 151.
12. J. Rodriguez-Carvajal, *Physica B (Amsterdam)*, 1993, 192, 55.
13. V. Trunov, A. Sokolov, V. Lebedev, O. Smirnov, A. Kurbakov, J. van den Heuvel, E. Batyrev, T. Yurieva, L. Plyasova, and Gy. Torok, *Preprint No. 2587, PNPI (St. Petersburg Institute of Nuclear Physics, Russian Academy of Sciences)*, 2004.
14. A. Guinier and G. Fournet, *Small-Angle Scattering of X-Rays (Wiley, New York)*, 1955.
15. R. Montarnal, *Diffusion in Catalysts with Bi-Dispersed Structure, in Porous Structure of Catalysts and Transfer Processes in Heterogeneous Catalysis (Nauka, Novosibirsk)*, 1970, 105.
16. D.I. Svergun, *J. Appl. Crystallogr.*, 1992, 25, 495.